

Biophysical Journal, Volume 97

Supporting Material

Factor Xa Binding to Phosphatidylserine-Containing Membranes Produces an Inactive Membrane-Bound Dimer

Tilen Koklic, Rinku Majumder, Gabriel E. Weinreb, and Barry R. Lentz

Abbreviations:

S-2238, H-D-phenylalanyl-L-pipecolyl-L-arginin-p-nitroanilid dihydrochlorid (synthetic substrate for thrombin);

S-2765, N- α -benzyloxycarbonyl-D-arginyl-L-glycyl-L-arginin-p-nitroanilid dihydrochlorid (synthetic substrate for factor Xa);

DOPC, 1,2-dioleoyl-3-sn-phosphatidylcholine;

PS, phosphatidylserine (porcine brain in this study);

Pre2, prethrombin 2 (catalytic domain of prothrombin);

Ila, thrombin;

FXa, factor Xa

Tris, tris(hydroxymethyl)aminomethane;

PEG 8000, poly(ethylene glycol);

SUV, small unilamellar vesicle

DEGR, Dansyl-GLU-GLY-ARG-chloromethylketone

FEGR, Fluorescein-GLU-GLY-ARG-chloromethylketone

DEGR-Xa, irreversibly inactivated factor Xa by alkylation of the active site histidine residue with DEGR

FEGR-Xa, irreversibly inactivated factor Xa by alkylation of the active site histidine residue with FEGR

EXPERIMENTAL PROCEDURES

Materials Human FXa, DEGR-Xa, FEGR-Xa, and prothrombin 2 (the catalytic domain of prothrombin with the R³²²-I³²³ bond intact; Pre2) were obtained from Hematologic Technologies Inc. (Essex Junction, VT). Pre 2 purity was checked by running it on a 10% PAGE Gel, where it showed a single band without any contamination of Frag1.2. FXa purity was verified by activity assay (1). The factor Xa-specific substrate N-2-benzyloxycarbonyl-D-arginyl-L-arginine p-nitroanilide dihydrochloride (S-2765) and thrombin (IIa)-specific substrate H-D-phenylalanyl-L-pipecolyl-L-arginine p-nitroanilide dihydrochloride (S-2238) were purchased from DiaPharma (W.Chester., Oh). Calcium chloride was reagent grade from Fisher Chemicals. 1,2-dioleoyl-3-sn-phosphatidylcholine (DOPC) and porcine brain phosphatidylserine (PS) were purchased from Avanti Polar Lipids (Alabaster, AL). Concentrations of the phospholipids were established by inorganic phosphate determination (2) and purity was tested by thin layer chromatography. All other chemicals were ACS reagent grade or the best available grade; all solvents were HPLC grade.

Methods.

Preparation of Phospholipid Vesicles: Small unilamellar vesicles (SUVs) composed of DOPC and PS in the molar ratio 75:25 were prepared in buffer A (see kinetic measurements) as described previously (3, 4).

Measurement of the Kinetics of Active Site Formation Using Synthetic Substrate: The activation of human Pre2 to thrombin was followed by measuring the generation of thrombin amidolytic activity against a synthetic substrate, S-2238. Pre2 activating mixtures contained Pre2, 25% PS membranes, and FXa in buffer A (50 mM Tris, 150 mM NaCl, 0.6% PEG, pH 7.4) and 1 or 4 mM Ca²⁺, at 37°C. The activation reaction was quenched at several time intervals (1, 2, 3, 4, 5, and 6 min) with 0.11 mg/mL (final concentration) soybean trypsin inhibitor (5). Aliquots of 5 µL of the quenched reaction mixture collected at different times were transferred into sample wells of a 96-well assay plate (Becton Dickinson, Oxnard, CA). The wells already contained 105 µL of buffer (50 mM Tris, 150 mM NaCl, 4 mM CaCl₂, and 0.6% PEG, pH 7.4) at 37 °C. An aliquot of 35 µL of the substrate S-2238 (0.47 mg/mL with 20 mM CaCl₂ at 37 °C) was added to this mixture. Following a brief mixing time (4 s), the absorbance at 405 nm was recorded using a tunable microplate reader (Versamax; Molecular Devices Corp., Sunnyvale, CA) so as to obtain the initial rate of S-2238 hydrolysis. The concentration of thrombin active site was determined by comparing the initial rate of S-2238 hydrolysis to a standard curve that had been generated using thrombin that was active site titrated with *p*-nitrophenyl *p*'-guanidinobenzoate (Sigma Chemical Co.) (6). The initial rates (R) of Pre2 activation were determined from plots of active site concentration versus time, which were linear in the time range examined (0-6 min). Kinetic data were analyzed according to the Michaelis-Menten formalism:

$$R = \frac{k_{cat} [X_a][P2]}{K_M + [P2]} \quad (1)$$

, where k_{cat} and K_M are the usual kinetic constants in this formalism, and $[X_a]$, and $[P2]$ are the concentrations of factor Xa and Pre2, respectively. For monomer FXa in solution,

R was linear in both [Xa] and [P2], demonstrating the second-order nature of Pre2 activation by monomer FXa and implying the validity of the Michaelis-Menten treatment. **Fluorescence measurements:** The fluorescence intensity of DEGR-Xa was recorded at 23°C with a Spex® FluoroLog-3 spectrofluorometer (Jobin Yvon Inc., Edison, NJ), using an excitation wavelength of 340 nm (band pass 2 nm) and emission wavelength of 550 nm (4-nm band pass). The excitation shutter was kept closed except during data collection to avoid photodegradation of the sample during all fluorescence measurements. Before every fluorescence titration, 100nM DEGR-Xa in a buffer B (20 mM Tris, 100 mM NaCl, pH 7.5) and either 2 mM (to match conditions of (7)) or 4 mM (to match conditions of our activity measurements) CaCl₂, at 23°C was incubated for ~50 min in a cuvette so as to condition the cuvette (8). After this initial incubation, the cuvette was rinsed with 2 mL of buffer B and fresh sample was added to the conditioned cuvette for measurements. Phospholipid membranes (25/75 PS/DOPC) were added in up to 4 μL aliquots, with a maximum volume dilution of 5%. We corrected for dilution by normalizing to the emission intensity of DEGR-Xa titrated by buffer alone. Fluorescence intensity was recorded ~2-3 min after each addition. Results were averaged as described previously (8).

The fluorescence lifetime of DEGR-Xa was recorded at 23°C with a MF² spectrofluorometer (Horiba Jobin Yvon Inc., Edison, NJ), using an excitation LED (Light Emitting Diode) with wavelength of 340 nm and emission cut off filter with wavelength of 500 nm. Before each titration, the cuvette was conditioned as described above. Phospholipid membranes containing 25% porcine brain PS and 75% DOPC were added in up to 4 μL aliquots, with a maximum dilution of 5%. Fluorescence lifetimes were recorded after ~2-3 min of equilibration following each membrane addition. The user-specified integration cycle at each membrane concentration was 6 min, during which phase shift and modulation ratio data were recorded at 16 frequencies between of 7 and 100 MHz (as shown in the inset of Figure 5). Results were analyzed using the Lifetime Modeling Application (version 2.2.12) from Jobin Yvon, Inc. (© 2003). We fitted both phase shift and modulation ratio data at each membrane concentration assuming the existence of three lifetimes (two were insufficient and fitting with four lifetimes gave ill-defined parameters). Fitting parameters were the lifetimes and fraction of each lifetime component contributing to the average lifetime. The lowest lifetime was roughly constant for all samples, but fixing this at its average value did not produce significantly better fits or better defined fitting parameters. The fluorescence anisotropy of FEGR-Xa was recorded at 23°C with a Spex® FluoroLog-3 spectrofluorometer (Jobin Yvon Inc., Edison, NJ), using an excitation wavelength of 490 nm (band pass 2.5 nm) and emission wavelength of 520 nm (band pass 2.5 nm). Phospholipid membranes (25/75 PS/DOPC) were added in up to 8 μL aliquots, with a maximum dilution of 5%. Fluorescence intensity was recorded ~2 min after each addition. Results were averaged 5 times or until a standard error of < 0.7% was achieved.

Global Analysis of data: To determine dimerization constants and activities of each FXa species several data sets were globally (simultaneously) fitted using Matlab 6.5 to numerically solve a system of coupled equations. The best fit parameters were found by minimizing the sum-of-squares of all data sets simultaneously.

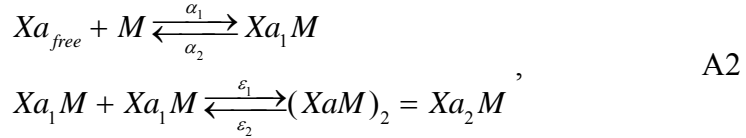
Appendix A: Analysis of FXa Activity (Figure 2) in The Presence of PS-Containing Membranes

Our treatment is based on the hypothesis that, in the presence of PS-containing membranes, FXa exists in three forms: monomer in solution, monomer on a membrane, and dimer on a membrane. The observed rate is then the sum of three rates:

$$R = [Xa_{free}] \times R_{free} + [XaM] \times R_1 + [Xa_2M] \times R_2 \quad A1$$

where R_{free} represents the rate of IIa formation by FXa in solution, R_1 is the rate of IIa formation by FXa bound on the membrane surface in monomer form (XaM), and R_2 is the rate of IIa formation catalyzed by FXa bound on the membrane surface in dimer form (Xa_2M). The rate of thrombin (IIa) formation from Pre2 as catalyzed by free FXa in solution is $R_{free} = k_{cat}/K_M \times [Pre2]$, where $k_{cat}/K_M = K^* = 94 \text{ M}^{-1}\text{sec}^{-1}$ (Figure 1). We do not know R_1 or R_2 , so these must be treated as adjustable parameters in our calculations.

The process that forms these three species involves two reactions, binding of FXa to PS-containing membranes and subsequent dimerization of FXa on a membrane:



where Xa_1M is membrane-bound FXa monomer, and Xa_2M is a membrane-bound FXa. It is presumed that the second equilibrium is established very rapidly. The first equilibrium is established less quickly but quickly enough that we can consider all three FXa species in equilibrium during the time course of our measurements. Thus,

$$[XaM]K_d^{Xa} = [Xa] \frac{[PL]}{N_{Xa}} \quad A3$$

$$[Xa_2M]_{\sigma} K_{d,\sigma}^{Xa_2} = [XaM]_{\sigma}^2 \quad A4$$

In Equation A3, $K_d^{Xa} = \frac{\alpha_2}{\alpha_1}$ is the equilibrium solution dissociation constant for FXa

binding to a membrane and N_{Xa} is the stoichiometry of membrane binding, *i.e.*,

$N_{Xa} = \frac{[PL]}{[M]}$ = the number of lipids involved in a FXa membrane binding site. In

Equation A4, $K_{d,\sigma}^{Xa_2} = \frac{\varepsilon_2}{\varepsilon_1}$ is the equilibrium *surface* dissociation constant of FXa

dimerization on a membrane. Note that $[XaM]$ is the molar concentration of membrane-bound FXa, but that $[XaM]_{\sigma}$ is the surface concentration of monomeric FXa and $[Xa_2M]_{\sigma}$ is the surface concentration of membrane-bound FXa dimer. Surface concentration is generally expressed as moles/area (we use mol/dm^2) but can equally well be expressed as a mol fraction, a unitless concentration that is that is a greatest theoretical relevance.

Since the total concentration of lipids and the total concentration of FXa are conserved, we can write two conservation equations:

$$\begin{aligned} [PL] &= [PL]_{tot} - N_{Xa} [XaM] - N_{Xa_2} [Xa_2M] \\ [Xa] &= [Xa]_{tot} - [XaM] - 2[Xa_2M] \end{aligned} \quad , \quad A5$$

where N_{Xa2} is the number of lipids contained in a FXa dimer binding site. In Equations A5, one must have all terms in the same concentration units. We can change units by recognizing that the total amount of surface-exposed lipid in the solution is $2/3 \times [PL_{tot}] \times V$, and thus that the total exposed surface area (S) is $\frac{2}{3} N_A S^* [PL]_{tot} V$, where S^* is the surface area of a single lipid and N_A is Avogadro's number. S^* varies with lipid species, temperature, pressure, salt conditions, *etc.*, although values between 60 and 70 \AA^2 are likely (9). Based on geometric considerations and the assumption of constant chain packing across the bilayer, the outer leaflet value for a small, unilamellar vesicle is thought to be somewhat greater (74 \AA^2) and the inner leaflet value smaller (61 \AA^2) (10). In the absence of hard data, we ignore this complication and assume a value of is 65 \AA^2 . With this value for S^* , $S \approx 2.6 \times 10^7 \text{ dm}^2 / \text{mol} [PL]_{tot} V$. The amounts of surface-bound monomer and dimer are $[XaM]V = [XaM]_{\sigma} S$ and $[Xa_2M]V = [Xa_2M]_{\sigma} S$, respectively, where V is the volume of the solution and S is the total surface area of phospholipid membrane in the solution. Using this, we can rewrite Equation A4 as:

$$[XaM]^2 = [Xa_2M] K_{dXa_2, \sigma} \frac{S}{V} = [Xa_2M] K_{dXa_2, \sigma} \frac{2}{3} S^* N_A [PL_{tot}] = [Xa_2M] K_{dXa_2} \quad A6$$

, where K_{dXa_2} is the dimerization constant expressed in solution units. Now, we substitute Equations A3 and A5 into A6 to obtain:

$$K_{dX_a} N_{X_a} [X_a M] - \left([X_{a, tot}] - [X_a M] - \frac{2[X_a M]^2}{K_{dX_a^2, \sigma} \frac{2}{3} N_A S_1 [PL_{tot}]} \right) \times \left(\frac{[PL_{tot}] - N_{X_a} [X_a M] - N_{X_a^2} [X_a M]^2}{K_{dX_a^2, \sigma} \frac{2}{3} N_A S_1 [PL_{tot}]} \right) = 0 \quad A7$$

In this expression, $[Xa_{tot}]$ and $[PL_{tot}]$ are experimental variables, while $K_{dX_a^2, \sigma}$ and N_{Xa_2} are unknown parameters. This is a 4th order polynomial in $[XaM]$ that has four roots, only one of which is physically reasonable with $[XaM] \leq [Xa_{tot}]$ and $[PL_{tot}]/N_{Xa}$. This root provides $[XaM]$ for a given $[Xa_{tot}]$ and $[PL_{tot}]$, and unknown parameters $K_{dX_a^2}$ and N_{Xa_2} . Equations A7 and A4 determine the remaining FXa species.

With the concentrations of all FXa species known one can evaluate activation rates using Equation A1. These can be compared to experimental rates to obtain R_1 , R_2 , $K_{dX_a^2}$ and N_{Xa_2} by minimizing the square deviation of R_{calc} from R_{obs} . The mole fractions of FXa in each of the three species present (free, bound monomer, and bound dimer) are also easily determined from $[Xa_{tot}]$, $[XaM]$, and $[Xa_2M]$.

We note that the surface dimerization constant is independent of lipid concentration, but the dimerization constant in solution units depends on lipid concentration. If the solution dimerization constant is expressed in the same units as $[PL]$, then the surface dimerization constant in surface units is related to the dimerization constant in solution units by

$$K_{dX_a^2} = K_{dXa_2, \sigma} \frac{2}{3} S^* N_A [PL_{tot}]; \text{ or } K_{dX_a^2, \sigma} = \frac{K_{dX_a^2}}{[PL]} 3.83 \times 10^{-10} \text{ mol} / \text{dm}^2 \quad A8$$

A valuable unit of concentration is mole fraction, since binding constants expressed in these units are unit-less and thus directly related to unitary free energies of

binding. We can also express the dimerization constant having solution units (M^{-1}) in mole-fraction units as:

$$K_{dX_a} = \frac{[X_a] \frac{[PL]}{N_{X_a}}}{[X_a PL]} = \frac{\frac{n_{X_a}}{V_o} \frac{1}{N_{X_a}} \frac{n_{PL}}{V_o}}{\frac{n_{X_a PL}}{V_o}} = \frac{x_{X_a} \frac{x_{PL}}{N_{X_a}}}{x_{X_a PL} [W]} = \frac{K_{dX_a, x}}{[W]}, \quad A9$$

where x_i is a mol fraction of i , defined as the number of moles n_i divided by the total number of moles of water in the system, n_w . $[W] = 55.3 M$ is the molar concentration of pure water. V_o is the total volume of the solution. This approximation is valid when the number of moles of water (solvent) in the system is much greater than the number of moles of solute n_i , and is therefore $n_i = \frac{n_i}{n_i + n_w} \approx \frac{n_i}{n_w}$.

Similarly, we convert the surface dissociation constant in units of $\text{mol}/(\text{dm})^2$ to mole-fraction units using:

$$K_{dX_a, \sigma} = \frac{[X_a PL]_{\sigma}^2}{[X_a^2 PL]_{\sigma}} = \frac{\left(\frac{n_{X_a PL}}{S_o} \right)^2}{\frac{n_{X_a^2 PL}}{S_o}} \approx \frac{n_{PL}}{S_o} \frac{\left(x_{X_a PL} \right)^2}{x_{X_a^2 PL}} = [PL]_{tot} \frac{V_o}{S_o} K_x = \frac{3}{2N_A S_0} K_x, \quad A10$$

where x_i is a mol fraction of i , defined as the number of moles of bound species, n_i , divided by the total number of moles of lipid molecules plus bound species in the system, $n_{PL} + \sum_i n_i$. In Equation A10, we make the approximation that $n_{PL} \approx n_{PL} + \sum_i n_i$, which is true in the case of a very dilute surface, namely when the number of moles of lipid in the system is much greater than number of moles of bound species, which is not always the case. S_o is the total surface area in the experiment. Avogadro's number N_A and the surface area of a lipid molecule, S^* , define the total exposed (outer leaflet) surface area of a mol of lipid incorporated into small, unilamellar vesicles, as used in our studies; $\frac{2}{3} N_A S^* = 2.6 \times 10^7 \text{ (dm)}^2 / \text{mol}$.

Appendix B: Analysis of The Fluorescence Intensity (FI) Signal of DEGR-Xa (Figure 3) in The Presence of PS-Containing Membranes

The fluorescence intensity (F) of DEGR-Xa in the presence of PS-containing membranes, to which DEGRXa can bind, consists of three terms:

$$F = F_{free} + F_{monomer} + F_{dimer}, \quad B1$$

where F_{free} represents the intensity of fluorescence signal of DEGRXa in solution,

$FI_{monomer}$ is the intensity of fluorescence signal of DEGR-Xa bound on the membrane surface in monomer form, and FI_{dimer} is the intensity of fluorescence signal of DEGR-Xa bound on the membrane surface in dimer form.

The fluorescence intensity signal from a DEGR-Xa species (F_i) depends on both the concentration ($[DEGR - X_a]_i$) and the intrinsic fluorescence intensity (f_i) of the species i :

$$F_i = f_i \times [DEGR - X_a]_i, \quad \text{B2}$$

The binding of DEGR-Xa to membranes and subsequent dimerization of DEGR-Xa on a membrane can be treated the same as binding and dimerization of FXa using the same set of equations discussed in Appendix A. The only difference was that measurements of activities all had associated uncertainties (σ) while fluorescence intensities were measured by photon counting and thus assigned uncertainties associated with a Poisson distribution ($\sigma = 1/\sqrt{\text{counts}}$).

Appendix C: Analysis of The Fluorescence Anisotropy (r) Signal of FEGR-Xa (Figure 4) in The Presence of PS-Containing Membranes.

Just like hetero-FRET, homo-FRET can yield an estimate of the distance between fluorophores. The fluorescence anisotropy from a cluster of two fluorescein molecules can be written (11)

$$r_{dimer} = r_1 \times \left(\frac{1 + (R_0/R)^6}{1 + 2 \cdot (R_0/R)^6} \right) + r_{et} \times \left(\frac{(R_0/R)^6}{1 + 2 \cdot (R_0/R)^6} \right), \quad \text{C1}$$

where r_{dimer} is the anisotropy from the cluster (dimer). In this expression, the first term is the anisotropy due to emission from the initially excited molecule, which is normally that of a monomer (r_1) but is reduced in a dimer due to excited state resonance between the two chromophores, the probability of which is expressed by the R_0/R term. The second term in this expression is due to emission from the acceptor molecule of a dimer. This is expected to be only 0.016 after a single energy transfer event even if excitation and emission dipoles are parallel and the two fluorescein molecules are held rigid, and is typically assumed to be much smaller (close to 0) when these two conditions are not met (11). The fluorescence anisotropies of the initially excited fluorophore would be those of monomer in solution or monomer on the membrane. The data in Figure 3C make it clear that these anisotropies are essentially equal and can be set to ~ 0.1595 . R_0 is the Förster distance for the fluorescein-fluorescein pair, which is a property of the electronic properties of the chromophores and the relative orientation of their emission and excitation dipoles and is variously given as 50 Å (12) to 56 Å (11), R is the separation distance between donor and acceptor. In our case, the fluorescence anisotropy is a sum of contributions of depolarization originating from free FEGR-Xa in solution, monomer bound on membranes, and dimers. In general, the total observed anisotropy of a system composed of several species is a sum of intensity-adjusted contributions of each species to the total anisotropy (13):

$$r = \sum_{i=1}^n Z_i \times r_i, \quad \text{C2}$$

where the intensity-adjusted mole fraction, Z_i , is given by:

$$Z_i = \frac{X_i}{X_i + \sum_{j \neq i}^n X_j \frac{F_j}{F_i}}, \quad \text{C3}$$

where F_i and X_i are fluorescence intensities and mol fractions, respectively, of free FEGR-Xa, FEGR-Xa monomers, or FEGR-Xa in dimers. Plots of the intensity of FEGR-Xa emission upon titration with PS-containing membranes (Figure 4B) show that $F_{\text{free}} \approx F_{\text{monomer}} \geq F_{\text{dimer}}$. With this assumption, we can rewrite equation C2 as:

$$r_{\text{obs}} = Z_{\text{free}} \times r_{\text{free}} + Z_{\text{monomer}} \times r_{\text{monomer}} + Z_{\text{dimer}} \times r_{\text{dimer}}, \quad \text{C4}$$

where expressions for X_{free} , X_{monomer} , and X_{dimer} are mole fractions of FEGR-Xa in each of three species. Taking into account that $X_{\text{dimer}} = 1 - X_{\text{monomer}} - X_{\text{free}}$, we can rewrite C3 as:

$$Z_{\text{free}} = \frac{X_{\text{free}}}{X_{\text{dimer}} (F_{\text{free}}/F_{\text{dimer}} - 1)}; Z_{\text{monomer}} = \frac{X_{\text{monomer}}}{X_{\text{dimer}} (F_{\text{free}}/F_{\text{dimer}} - 1)}; Z_{\text{dimer}} = \frac{X_{\text{dimer}} (F_{\text{free}}/F_{\text{dimer}})}{X_{\text{dimer}} (F_{\text{dimer}}/F_{\text{free}} - 1) + 1}. \quad \text{C5}$$

Similarly, we can express the fluorescent intensity of FEGR-Xa (Figure 4B) as:

$$F_{\text{obs}} = (1 - X_{\text{dimer}})F_{\text{free}} + X_{\text{dimer}}F_{\text{dimer}}; \frac{F_{\text{obs}}}{F_{\text{free}}} = (1 - X_{\text{dimer}}) + X_{\text{dimer}} \left(\frac{F_{\text{dimer}}}{F_{\text{free}}} \right) \quad \text{C6}$$

X_{free} , X_{monomer} , and X_{dimer} can be obtained from the dimer model (Appendix A) if we know $K_{d,Xa}$ and $K_{d, \text{Surface}}^{\text{dimer}}$ and $r_{\text{free}} = r_{\text{monomer}} = 0.1595$. Thus, we can describe the data in both frames of Figure 4 in terms of the dimer model with four unknown parameters: $K_{d,Xa}$, $K_{d, \text{Surface}}^{\text{dimer}}$, $F_{\text{dimer}}/F_{\text{free}}$, and r_{dimer} , where r_{dimer} is the emission anisotropy of dimer, which can be related to R through equation C1. In order to reduce the parameters by one, we took the dissociation constant for monomer FEGR-Xa binding to a membrane as that obtained from Figure 3 for DEGR-Xa.

Acknowledgements

This work was supported by grant from the NHBL (HL 072827 to BRL). We gratefully acknowledge the help of Jim Mattheis, from HORIBA Jobin Yvon, Inc., with fluorescence life-time measurements and are thankful for the opportunity to work with pre release version of FluoroMax®-4.

REFERENCES:

1. Koppaka, V., J. Wang, M. Banerjee, and B. R. Lentz. 1996. Soluble phospholipids enhance factor Xa-catalyzed prothrombin activation in solution. *Biochemistry* 35:7482-7491.
2. Chen, P. S., Jr., T. Y. Toribara, and H. Warner. 1956. Microdetermination of Phosphorus. *Analytical Chemistry* 28:1756-1758.
3. Lentz, B. R., T. J. Carpenter, and D. R. Alford. 1987. Spontaneous fusion of phosphatidylcholine small unilamellar vesicles in the fluid phase. *Biochemistry* 26:5389-5397.
4. Majumder, R., M. A. Quinn-Allen, W. H. Kane, and B. R. Lentz. 2005. The phosphatidylserine binding site of the factor Va C2 domain accounts for membrane binding but does not contribute to the assembly or activity of a human factor Xa-factor Va complex. *Biochemistry* 44:711-718.
5. Bevers, E. M., J. Rosing, and R. F. Zwaal. 1986. Membrane phospholipids are the major determinant of the binding site for factor X activating--and prothrombinase complexes at the surface of human platelets. *Agents and actions* 20:69-75.
6. Chase, T., Jr., and E. Shaw, editors. 1970. *Titration of Trypsin, Plasmin, and Thrombin with p-Nitrophenyl p-Guanidinobenzoate HCl*. Academic Press, Inc.
7. Husten, E. J., C. T. Esmon, and A. E. Johnson. 1987. The active site of blood coagulation factor Xa. Its distance from the phospholipid surface and its conformational sensitivity to components of the prothrombinase complex. *J Biol Chem* 262:12953-12961.
8. Majumder, R., G. Weinreb, X. Zhai, and B. R. Lentz. 2002. Soluble Phosphatidylserine Triggers Assembly in Solution of a Prothrombin-activating Complex in the Absence of a Membrane Surface. *J. Biol. Chem.* 277:29765-29773.
9. Koenig, B. W., H. H. Strey, and K. Gawrisch. 1997. Membrane lateral compressibility determined by NMR and x-ray diffraction: effect of acyl chain polyunsaturation. *Biophys J* 73:1954-1966.
10. Huang, C., and J. T. Mason. 1978. Geometric packing constraints in egg phosphatidylcholine vesicles. *Proc Natl Acad Sci U S A* 75:308-310.
11. Runnels, L. W., and S. F. Scarlata. 1995. Theory and application of fluorescence homotransfer to melittin oligomerization. *Biophys J* 69:1569-1583.
12. Chen, L., Q. Yao, K. Brungardt, T. Squier, and D. Bigelow. 1998. Changes in Spatial Arrangement between Individual Ca-ATPase Polypeptide Chains in Response to Phospholamban Phosphorylation *Ann NY Acad Sci* 853.
13. Lentz, B. R., Y. Barenholz, and T. E. Thompson. 1976. Fluorescence depolarization studies of phase transitions and fluidity in phospholipid bilayers. 2 Two-component phosphatidylcholine liposomes. *Biochemistry* 15:4529-4537.